Journal of Biomedical Optics

SPIEDigitalLibrary.org/jbo

Enhanced photocoagulation with catheter-based diffusing optical device

Hyun Wook Kang
Jeehyun Kim
Jungwhan Oh

SPIE

Enhanced photocoagulation with catheter-based diffusing optical device

Hyun Wook Kang,[a] Jeehyun Kim,[b] and Jungwhan Oh[a]
[a]Pukyong National University, Department of Biomedical Engineering, 45 Yongso-ro Nam-gu, Busan, 608-737, Republic of Korea
[b]Kyungpook National University, School of Electrical Engineering and Computer Science, 1370 Sankyuk-dong, Buk-gu, Daegu, 702-701, Republic of Korea

Abstract. A novel balloon catheter-based diffusing optical device was designed and evaluated to assist in treating excessive menstrual bleeding. A synthetic fused-silica fiber was micro-machined precisely to create scattering segments on a 25 mm long fiber tip for uniform light distribution. A visible wavelength ($\lambda = 532$ nm) was used to specifically target the endometrium due to the high vascularity of the uterine wall. Optical simulation presented 30% wider distribution of photons along with approximately 40% higher irradiance induced by addition of a glass cap to the diffuser tip. Incorporation of the optical diffuser with a polyurethane balloon catheter considerably enhanced coagulation depth and area (i.e., 3.5 mm and 18.9 cm^2 at 1 min irradiation) in tissue *in vitro*. The prototype device demonstrated the coagulation necrosis of 2.8 ± 1.2 mm ($n = 18$) and no thermal damage to myometrium in *in vivo* caprine models. A prototype 5 cm long balloon catheter-assisted optical diffuser was also evaluated with a cadaveric human uterus to confirm the coagulative response of the uterine tissue as well as to identify the further design improvement and clinical applicability. The proposed catheter-based diffusing optical device can be a feasible therapeutic tool to photocoagulate endometrial cell layers in an efficient and safe manner. [DOI: 10.1117/1.JBO.17.11.118001]

Keywords: optical diffuser; endometrial coagulation; balloon-catheter; photocoagulation; myometrium; coagulation necrosis.

Paper 12495 received Aug. 3, 2012; revised manuscript received Oct. 4, 2012; accepted for publication Oct. 23, 2012; published online Nov. 15, 2012.

1 Introduction

Menorrhagia [also called abnormal uterine bleeding (AUB)] is an abnormality of having excessive bleeding from the uterus during a woman's menstrual cycle. On average, 30% of women are affected by heavy uterine bleeding at some time in their lifetime.[1,2] Symptoms of menorrhagia may include heavy (more than 80 ml blood loss), prolonged (more than seven days), or irregular periods.[3,4] Women with menorrhagia can be treated medically with oral contraceptive pills, nonsteroidal anti-inflammatory drugs, and androgenic steroids.[5] However, these medications are often associated with various side effects as well as temporary relief.[4,5] In order to seek a more permanent solution, surgical treatment alternatives have also been performed. A definitive treatment for AUB and other gynecological diseases is a hysterectomy, removal of the uterus. Nevertheless, the procedure is quite radical and invasive, with possible accompanying hemorrhage, long recovery time, high infection rate, bowel obstruction, and even sudden hormonal change; thus, patients with menorrhagia often pursue alternatives to hysterectomy.[6]

As a less invasive treatment option, hysteroscopic endometrial ablation has instead been performed to treat AUB by using a number of techniques such as thermal balloon, cryotherapy, bipolar radiofrequency, and microwave ablation.[4,7–10] Endometrial hyperplasia is one of the major causes of heavy menstrual bleeding. Thus, throughout the ablative techniques, the endometrium, which is the innermost layer of the uterus, is surgically removed to curb heavy bleeding without damaging the smooth muscle layer underneath the endometrium (myometrium) in order to maintain fertility. In spite of minimally invasive procedures, these treatments are still technically difficult and may result in thermal injury to peripheral tissue, eventually leading to various complications and unwanted sterility.[10] In addition, the procedures require a series of treatments (at least 10 min) to complete endometrial ablation, postoperatively leaving severe pain. Evidently, surgeons still need a way to complete endometrial destruction without the need for general anesthesia, surgical intervention, and complications.

Due to their high degree of accuracy and safety, fiber-based lasers have proved to be useful tools to ablate the endometrium with varying degrees of success.[11–13] A variety of wavelengths, including 805 nm (diode), 1064 nm (Nd:YAG), 1320 nm (Nd:YAG), and 2.12 μm (Ho:YAG), have been used for endometrial ablation.[11–13] Through direct irradiation of optical energy, the endometrium can be coagulated due to light absorption and resultant heat accumulation, leading to coagulation necrosis. The diode laser presented overall tissue effects similar to those of Nd:YAG lasers, both experimentally and clinically in light of tissue necrosis.[11] However, low absorption coefficients, particularly at near-IR (1064 and 1320 nm), resulted in deep optical penetration depth up to 5 mm in soft tissue (for water, optical penetration depth = 1/absorption coefficient = $1/0.1\ cm^{-1} = 10$ cm) and thus irreversible thermal damage into the deep tissue, entailing hemorrhage at the surface of the uterus.[12,13] In addition, the lasers (805, 1064, and 1320 nm)

Address all correspondence to: Jeehyun Kim, Kyungpook National University, School of Electrical Engineering and Computer Science, 1370 Sankyuk-dong, Buk-gu, Daegu 702-701, South Korea. Tel: 82 53 950 7221; Fax: 82 53 950 7229; E-mail: jeehk@knu.ac.kr, or Junghwan Oh, Pukyong National University, Department of Biomedical Engineering, 45 Yongso-ro, Nam-gu, Busan 608-737, South Korea. Tel: 82 51 629 5771; Fax: 82 52 629 5779; E-mail: jungoh@pknu.ac.kr

0091-3286/2012/$25.00 © 2012 SPIE

were operated in the continuous wave (CW) mode, so irreversible thermal injury was aggravated by protracted irradiation time (up to 10 min) and long heat diffusion. Under the irrigation environment, the mid-IR wavelength (2.12 μm) was readily associated with transmission loss on account of saline absorption (absorption coefficient = 70 cm^{-1}), so the laser would require higher input power for efficient light delivery.[12] Furthermore, end-firing fibers could hardly achieve uniform tissue coagulation due to their small numerical aperture to cover the endometrium surface and difficulty in maneuvering the fiber during laser ablation.[12]

In an attempt to obtain homogeneous light distribution, an optical diffuser has been developed and evaluated for endometrial ablation.[14–18] The diffuser was created by removing the cladding and adding a diffusing medium such as silicon and scattering particles on the core surface. However, the applied power level (≤25 W) was relatively lower than the requirement for surgical tissue removal, in that most applications were related to photodynamic therapy (PDT). In addition, the procedure was cumbersome because it required long irradiation time as well as administration of photosensitizers into a body prior to the operation, in comparison with surgical treatments. To prevent the risk of melting a diffuser, particularly under high power application, a balloon catheter was also developed and used together with a near-IR laser for treatment.[13] Since the laser heated the balloon material directly rather than the targeted tissue, indirect heating was induced to the endometrium layer, which needed the real-time monitoring of temperature inside the tissue with thermocouples for safety purpose. Additionally, a 1064 nm wavelength with deep optical penetration (~5 mm) at lower power (20 W) contributed to long irradiation time (10 to 12 min), deep coagulation necrosis (up to 4 mm), and undesirable hemorrhage.[13,19]

In the current study, an endoscopic optical diffuser was designed and developed for minimally invasive endometrial ablation with a visible wavelength. Due to high vasculature in the uterus,[20] a wavelength of 532 nm was selected to directly target blood vessels (hemoglobin) and glandular tissue in the endometrium and, in essence, to treat menorrhagia. A 1-mm core fiber was directly micro-machined to create scattering segments for light diffusion. The balloon catheter was incorporated with the diffuser in order to achieve fast and uniform heat distribution as well as to provide structure integrity during the treatment. Light propagation from the diffuser was optically simulated, and the designed diffusing device was evaluated *in vitro* and *in vivo* in terms of coagulation time and necrosis thickness. The prototype device was also validated with a cadaveric human uterus to see its clinical applicability.

2 Materials and Methods

2.1 *Fiber Fabrication and Simulation*

Figure 1 presents images of a fabricated diffusing fiber tip for endometrial treatment. For simple and reliable machining purposes, a 1-mm core diameter, synthetic-fused silica (Suprasil 312, Heraeus Quarzglas GmbH & Co. KG, Germany) was selected to transmit the visible laser light (λ = 532 nm). Initially, the fiber cladding was removed mechanically, and the surface of the fiber core at the 25 mm distal end was circumferentially micro-machined by a 30 W CO_2 laser (λ = 10.6 μm, Synrad, Mukilteo, WA, USA) in a predetermined zigzag pattern.[21] A series of scattering segments (approximately 50 μm in size) were created on the fiber surface to diffuse the laser light radially in all directions. In order to achieve the constant size of the scattering segments, the fiber tip was tapered down to 0.5 mm in diameter at the distal end [i.e., minimum diameter for currently reliable manufacturability; Fig. 1(a)]. Then, the diffusing tip was covered with a 27-mm long glass (2 mm outer diameter) cap to attain wide and uniform light diffusion as well as to protect the bare fiber tip during laser treatment, as shown in Fig. 1(b).

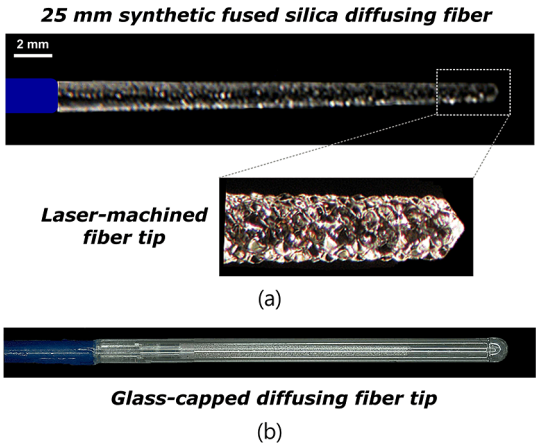

Fig. 1 Diffusing fiber tip for endometrial treatment: (a) 25 mm long tapered bare core (fused silica, 1 mm in diameter) after CO_2 laser micro-machining (each scattering segment of ~50 μm) and (b) glass-capped diffusing fiber tip for wide and uniform photon distribution.

In an attempt to predict photon distribution from the designed diffusing tip, optical simulation (Radiant Zemax, Redmond, WA, USA) was conducted to demonstrate light intensity and its spatial distribution at various distances. Two fiber conditions were compared: a bare diffuser tip (without a glass cap) and a glass-capped diffuser tip. To model the light scattered from the fiber surface, a Lambertian diffuser model was used with one million of rays and a light source with uniform angular distribution.[22] The diffusing tip was exclusively modeled with surface scattering (i.e., ~50 μm size scattering segment). The applied wavelength was 532 nm with the input power of 120 W, and the entire fiber length was 1.5 m including a 25 mm diffusing part at the tip. A 40 × 50 mm planar detector was placed underneath the diffusing fiber at distances of 1, 5, and 10 mm to identify light propagation and the spatial distribution of the scattered photons in two-dimensional (2-D). The profiles of light intensity (i.e., irradiance, W/cm^2) were also measured and quantitatively compared between the two fiber conditions.

2.2 *In Vitro Experiments*

Bovine liver tissue was used as a tissue model for *in vitro* tests with the designed diffusing fibers, in that the chromophores, such as dead endothelial cells and blood vessels, would still be able to absorb the visible laser light (λ = 532 nm) significantly.[23,24] The liver specimens were acquired from a local slaughter house, and they were cut into 5 × 7 cm segments in size (approximately 1 cm thick) and stored at 4°C prior to the experiments. Figure 2(a) illustrates an experimental set-up of photocoagulation tests with the fibers. A circular tissue holder (7 cm in diameter and 1 cm in thickness) was prepared, and a 1 cm thick tissue sample was placed at the bottom of the holder

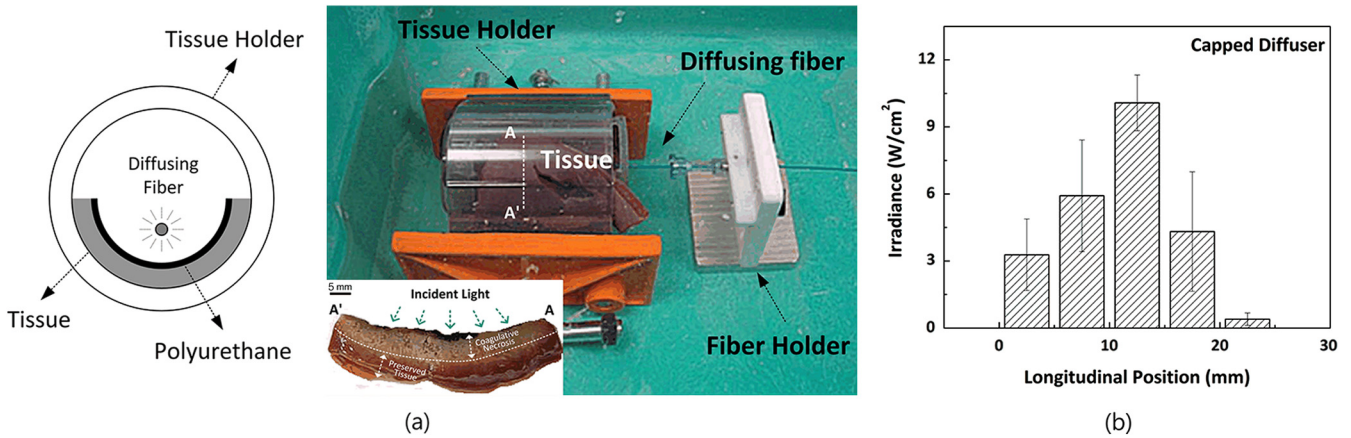

Fig. 2 *In vitro* photocoagulation test: (a) experimental set-up (cross-sectional view of diffusing light set-up, left image; tissue encased by tissue holder and fiber placed along tissue, right image; cross-sectional image (*A*-*A*′) of coagulated tissue, bottom of right image) and (b) intensity profile measured from 25 mm capped diffusing fiber tip.

along the curvature. The curved surface of the tissue sample partially reflected the transverse anatomic features of human uterus [Fig. 2(a)]. The diffusing fiber was located 1 cm above the tissue surface, so the incident light was uniformly irradiated on the tissue due to the curved geometry of the sample. A conventional clinical laser ($\lambda = 532$ nm, quasi-cw mode, High Performance System, CA, USA) was employed for laser coagulation, and the input power was maintained at 120 W in order to entail tissue coagulation through the diffusing tip. The average irradiance on the tissue surface was calculated to be approximately 3.8 W/cm^2. Three fiber conditions were tested: bare diffusing fiber, capped diffusing fiber, and capped diffusing fiber with a 1 mm thick layer of polyurethane (PUR). As PUR is a raw material for balloon catheters for endoscopic applications,[25] so the last condition represented the final device design to incorporate the capped diffusing fiber into a balloon catheter. However, for the sake of experimental simplicity, a thin layer of PUR was placed on top of the target tissue [Fig. 2(a)] instead of using a balloon catheter. During the tests, a PUR layer was superimposed upon the tissue sample as shown in Fig. 2(a) (left image). Prior to coagulation tests, the optical transmission of each fiber (bare diffusing, capped diffusing, and capped diffusing with a PUR layer) was roughly measured with a photodetector to be 99%, 97% and 94.5%, respectively. Figure 2(b) presents the intensity profile along the capped fiber tip that was measured every 5 mm. In addition, the transmission loss of PUR at 532 nm was measured with the detector to be less than 2.5%, which experimentally verified negligible light absorption (i.e., optically transparent with no light scattering) at 532 nm by the PUR layer. The coagulation threshold was preliminarily determined for the three fiber conditions by varying irradiation times from 2 to 8 s (1 s increments; a sample per each condition). The onset of visible discoloration on tissue surface was considered the physical evidence of coagulation. A number of irradiation times (4, 7, 15, 30, 60, 90, 120, 150, and 180 s) were then evaluated for the three conditions to identify the temporal evolution of photocoagulation on the tissue surface. Due to difficulty of preparing fresh tissue specimens with a large uniform surface area, each condition was tested only with a single liver sample for evaluating surface coagulation. All the specimens were placed under saline environment (room temperature) during the laser irradiation, and the temperature of the liver tissue was maintained at approximately 20°C. Postexperimentally, the radial depth (i.e., into the tissue) and 2-D area of coagulation on the tissue surface were quantified and compared with an image processing software tool (Image J, National Institute of Health, MD, USA). The image in Fig. 2(a) (bottom of the right image) showed a cross-sectional part of the photocoagulated tissue. In order to measure coagulation thickness, each irradiated specimen was cross-sectioned into three pieces [Fig. 2(a)], and the coagulation thickness of each piece was measured five times ($n = 15$). The discolored zone (tan color) represented coagulation necrosis and the red color was the preserved native tissue. A two-tailed Student's *t*-test was used for statistical analysis and $p < 0.05$ meant statistically significant.

2.3 *In Vivo and Cadaver Experiments*

Three mature female Saanen goats were used for *in vivo* retrograde laser coagulation studies. Animal procedures and care were conducted in accordance with a protocol approved by American Preclinical Service (APS) Institutional Animal Care and Use Committee (IACUC). Experiments, necropsy, and histology were performed at APS,[12] and all surgical procedures were performed with the animals under general endotracheal anesthesia. A caprine uterus is typically bicornuate so two prominent uterine horns come together to form a short uterine body.[26–28] Thus, six caprine uteri in total were tested for the current photocoagulation tests. Similar to a human uterus, the caprine uterine wall consists of two major tissue layers: endometrium and myometrium.[27,28] The endometrium is a pseudostratified layer of epithelium on the luminal surface of the uterus, containing richly vascular loose connective tissue along with fibroblasts, macrophages, and mast cells. The myometrium is two layers of smooth muscle separated by the stratum vasculare, which is a zone of large vessels (arteries, veins, and lymph vessels). For the current *in vivo* studies, the prototype device was evaluated to photocoagulate solely the endometrial layer, in that any thermal injury to the myometrium would adversely affect fertility. The prototype device consisted of a capped diffusing fiber, a PUR balloon catheter, a customized inflating tube (1 cm outer diameter and 8 cm long), and a customized inflating pump (variable pressure levels from 1 to 7 psi). The 4-cm long catheter device was inserted into the animal uterus, and the balloon catheter was distended with saline until it securely held the uterine wall (i.e., approximately 3 cm in balloon diameter at

5 psi). A 532 nm clinical laser was used with the input power of 120 W, and the irradiation time was approximately 30 s, based upon *in vitro* results (i.e., applied energy = 3600 J and irradiance = 3.2 W/cm^2 assuming a 3-mm thick endometrium for photocoagulation). Postoperatively, all the animals were euthanized 2 h after the tests by euthasol injection. Immediately after euthanasia, each uterine horn was removed, fixed in 10% neutral buffered formalin, and embedded in paraffin for hematoxylin and eosin (H&E) staining. From histology images, the thickness of coagulation necrosis was measured with Image J($n = 18$) and evaluated quantitatively.

A human uterus was donated by a 59-year-old postmenopausal patient for research at APS after a radical hysterectomy. The cadaveric uterus was used to evaluate the feasibility of the prototype device in terms of light leaking and deployment of fiber and balloon during laser irradiation. The device was inserted through the cervix for minimally invasive uterine access, and a 5-cm long balloon catheter was distended at 4 psi by saline (approximately 1.8 cm in balloon diameter). The applied power of 120 W was irradiated on the uterine wall for approximately 20 s (i.e., applied energy = 2400 J and irradiance = 4.2 W/cm^2) as the distance between the fiber and tissue was closer than the *in vivo* condition due to the rigidity of the cadaveric tissue. The degree of coagulation necrosis in the tissue was also examined postexperimentally with Image J($n = 12$). A digital camera (9.1M DSC-H50, Sony Corp, Japan) was used to take images of pre-, intra-, and postoperation to show a sequence of photocoagulation. A two-tailed Student's *t*-test was also used for statistical analysis and $p < 0.05$ meant statistically significant.

3 Results

3.1 *Optical Simulation*

Figure 3 shows the spatial distribution of photons from optical simulation comparing diffusing and capped diffusing fibers at various distances of 1, 5, and 10 mm. At 1 mm, both fibers created similar photon distributions with generation of high irradiance along the fiber due to their close proximity to a planar detector. However, as the distance from the detector increased up to 10 mm, the distribution became wider due to light diffusion from scattering segments on the fiber surface. The diffusing fiber presented elongated shape (along z axis) with relatively lower irradiance whereas the capped diffusing fiber created relatively circular distribution with higher irradiance, resulting from additional beam diffraction (along x axis) through the glass cap [Fig. 3(a)].

At a distance of 10 mm, longitudinal and horizontal distributions of the incident photons were compared in Fig. 3(b). Both directions demonstrated that the capped diffusing fiber yielded approximately 40% higher irradiance than the diffusing fiber (i.e., peak intensity = 10.8 W/cm^2 for the capped diffusing versus 7.7 W/cm^2 for the diffusing fiber). Based upon the longitudinal position, the width of the irradiance distribution was comparable between the two cases [Fig. 3(b)]. However, the capped diffusing fiber created around 30% wider horizontal distribution of the irradiance (i.e., Full-width-half-maximum = 15.2 mm for the capped diffusing versus 11.5 mm for the diffusing fiber). According to the simulation results, an additional layer from the glass cap circumscribed the longitudinal photon distribution and contributed to uniformly distribute the incident photons along x-axis.

3.2 *In Vitro Results*

Figure 4 demonstrates the progression of laser-induced coagulation on tissue as a function of irradiation time for three fiber conditions: diffusing, capped diffusing, and capped diffusing fiber with PUR. The total applied energy (i.e., 120-W input power times irradiation time) was 840, 3600, 7200, and 14,400 J at 7, 30, 60, and 120 s, respectively. Overall, the degree of photocoagulation on the tissue surface developed gradually with the irradiation time. Coagulation initially developed in a vertical direction (i.e., perpendicular to the fiber axis) and later expanded horizontally (i.e., along the fiber axis) with the irradiation time. The shape of the coagulated area was almost rectangular for the three conditions, and at 120 s the area length (i.e., perpendicular to the fiber axis) and width (i.e., along the fiber axis) were measured to be 3.1 and 2.5 cm, respectively. In other words, the area length was equivalent to the length of the half arc length of the diffusing light 1 cm away from the fiber (i.e., $\pi \times 1$ cm distance), and the area width became equivalent to the length of the diffusing fiber tip (~25 mm). Compared to the diffusing and capped diffusing fibers, the last condition (capped diffusing fiber with PUR) overtly yielded more rapid and wider tissue coagulation (i.e., 9.6 cm^2 for the last condition versus 0 cm^2 for diffusing fiber and 5.2 cm^2 for capped diffusing fiber at 7 s after irradiation). In fact, the coagulated area for the last condition became rapidly saturated after 30 s, compared to the two other conditions.

Figure 5(a) shows the quantitative evaluation of coagulation depth in a radial direction (into the tissue) as a function of irradiation time. For a diffusing fiber, coagulation threshold time was around 7 s, whereas coagulation for two other conditions was initiated around 4 s after irradiation (coagulation thickness = 100 to 200 μm). Similar to Fig. 4, a capped diffusing fiber with PUR increased the coagulation depth more rapidly than the other conditions. In the case of 1-min irradiation, the capped fiber with PUR created the coagulation necrosis of 3.5 ± 0.3 mm, which was 5-fold and 1.5-fold thicker than the diffusing (0.7 ± 0.2 mm) and capped diffusing fibers (2.5 ± 0.3 mm), respectively [$p < 0.001$; Fig. 5(a)].

Figure 5(b) demonstrates the progression of coagulation area on the tissue surface that indicated lateral thermal expansion. The diffusing fiber presented that coagulation area increased almost linearly with the irradiation time as coagulation depth did in Fig. 5(a). On the other hand, for both capped diffusing fiber and capped diffusing fiber with PUR, the coagulation area initially increased but became saturated approximately 1 min after irradiation, whereas the overall tendency of the coagulation depth almost linearly increased with time for both cases. At 1-min irradiation, the capped diffusing fiber with PUR condition yielded 3.8-fold and 1.6-fold larger coagulation areas than the diffusing and capped diffusing fibers, respectively (i.e., 18.9 cm^2 for capped diffusing fiber with PUR versus 5.0 cm^2 for diffusing and 11.7 cm^2 for capped diffusing fibers).

3.3 *Prototype and In Vivo Results*

After *in vitro* validation of various diffusing fiber conditions, the design for the capped diffusing fiber was finalized, and the prototype optical device was made and incorporated with a balloon catheter for *in vivo* and cadaver studies as shown in Fig. 6(a). The capped diffusing fiber was placed in the center of an 8 cm long (1 cm in outer diameter) customized inflating tube [inset of Fig. 6(a)], of which the proximal end was connected to a

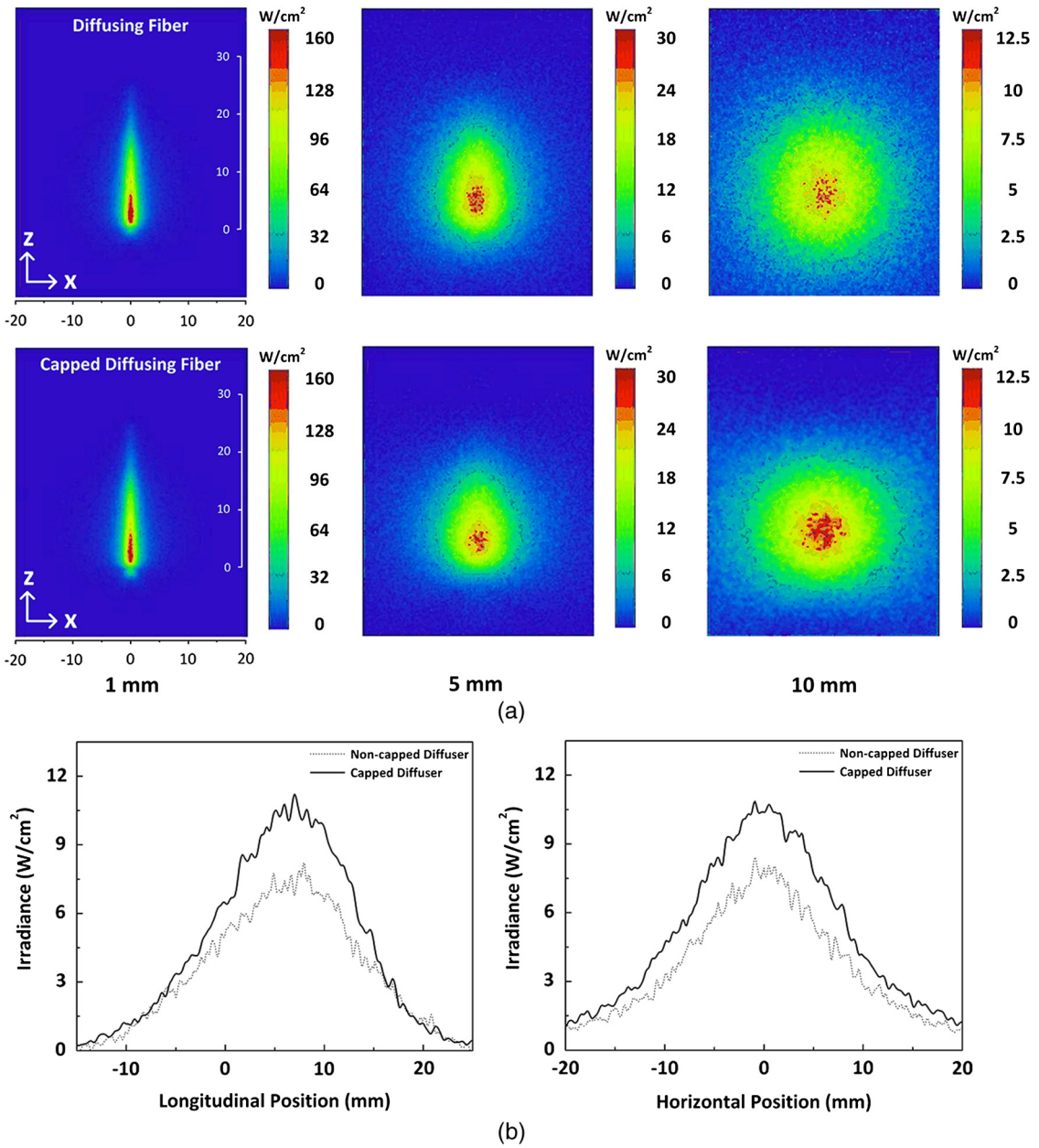

Fig. 3 Simulated photon distribution from newly designed diffuser tip at various distances (1, 5, and 10 mm): (a) 2-D spatial distribution of irradiance for diffusing fiber (top) and capped diffusing fiber (bottom) and (b) longitudinal (along z-axis at $x = 0$ mm) and horizontal (along x-axis at $z = 10$ mm) irradiance distribution measured at 10 mm distance. Note that the distal end of each fiber was placed at $x = 0$ and $z = 25$ mm and a 40×50 mm planar detector was used.

customized inflating pump (variable pressure levels from 1 to 7 psi) to regulate the input pressure for saline supply. The distal end of the fiber tip was insecurely positioned (i.e., free end) inside the balloon. A 4 cm long PUR-based balloon catheter was tightly attached to the distal end of the inflating tube, and the size of the balloon was adjustable, depending upon the geometry of uterus and pump pressure levels. In order to distend the balloon catheter, saline was pumped through the tube to fill out the balloon until the target uterus was securely fixed for laser surgery. Prior to *in vivo* tests, the prototype was validated to ensure the tight sealing of the catheter connection at the distal end of the tube.

Figure 6(b) shows the acute thermal response of a caprine uterine horn tissue 2 h after a 30 s coagulation with the prototype device (applied energy = 3600 J and irradiance = 3.2 W/cm^2). After 30 s irradiation, photocoagulation entailed the uniform coagulation necrosis on the treated tissue, which appeared as the shape of the distended (i.e., 3 cm wide and 4 cm long due to the size of caprine uterus) balloon catheter [inset of Fig. 6(b)]. The overall thickness of coagulation necrosis was measured to be 2.8 ± 1.2 mm ($n = 18$), which was slightly thinner than the estimated thickness (3 mm) of the distended uterine wall ($p = 0.53$). No hemorrhage occurred in both endometrium and myometrium after the laser treatment. Figure 7 presents H&E-stained histology images of the laser-treated uterine tissue. Treatment sites were readily identified by the presence of endometrial gland changes, edema, endometrial connective tissue changes, and vacuolation of smooth muscle

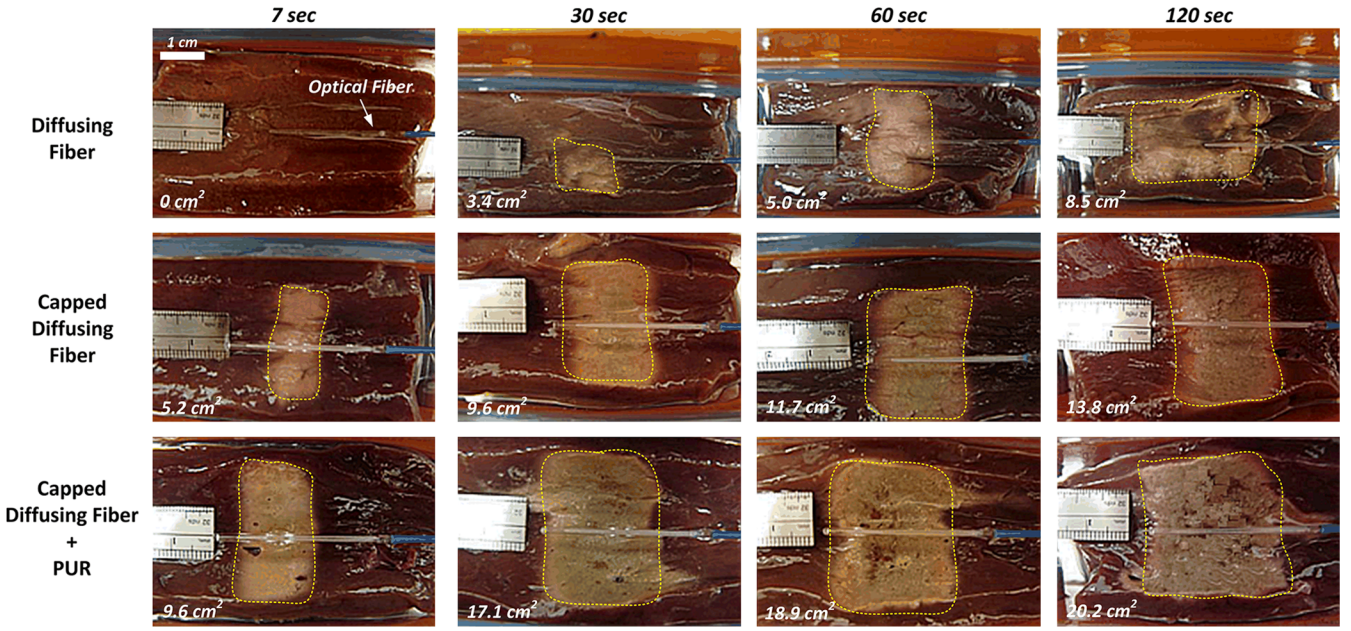

Fig. 4 Series of images of photocoagulated tissues at various irradiation times: diffusing fiber (top), capped diffusing fiber (middle), and capped diffusing fiber with polyurethane (PUR) layer (bottom). Note that each number in the left corner (cm^2) represents coagulated area (dotted in tissue), respectively.

cells in myometrium.[29] The balloon-contacted tissue was merely coagulated without any thermal injury to adjacent tissue [Fig. 7(a)], in that endometrial glands, as well as the superficial epithelial lining on the luminal surface, were markedly obliterated along with sloughed epithelium. The coagulation process was also evidenced by protein coagulum created on the endometrium surface [Fig. 7(b)], smeared or atypical appearing epithelial cells [Fig. 7(c)], and amphophilic connective tissue surrounding vessels [Fig. 7(c)]. It was confirmed in Fig. 7(d) that the myometrial smooth muscle adjacent to the treatment site yielded minimal changes, such as cellular vacuolation (solid line) and slight discoloration (dotted line), representing no overt thermal damage or necrosis to the myometrium.

3.4 *Cadaver Study*

Followed by *in vivo* studies, a cadaveric human uterus was tested with the prototype device (applied energy = 2400 J and irradiance = 4.2 W/cm^2; Fig. 8). Unlike the *in vivo* caprine studies, a slightly longer balloon catheter (i.e., 5 cm long versus 4 cm long for *in vivo*) was used for the larger size of the human uterus [Fig. 8(a)]. However, due to the rigidity of the cadaveric tissue, the balloon was distended only up to 1.8 cm in diameter; accordingly, the irradiation time was limited to approximately 20 s (i.e., 30% shorter than the irradiation time for *in vivo* study, 30 s) because of the closer irradiation distance between the fiber and endometrial luminal surface (i.e., 0.9 cm for

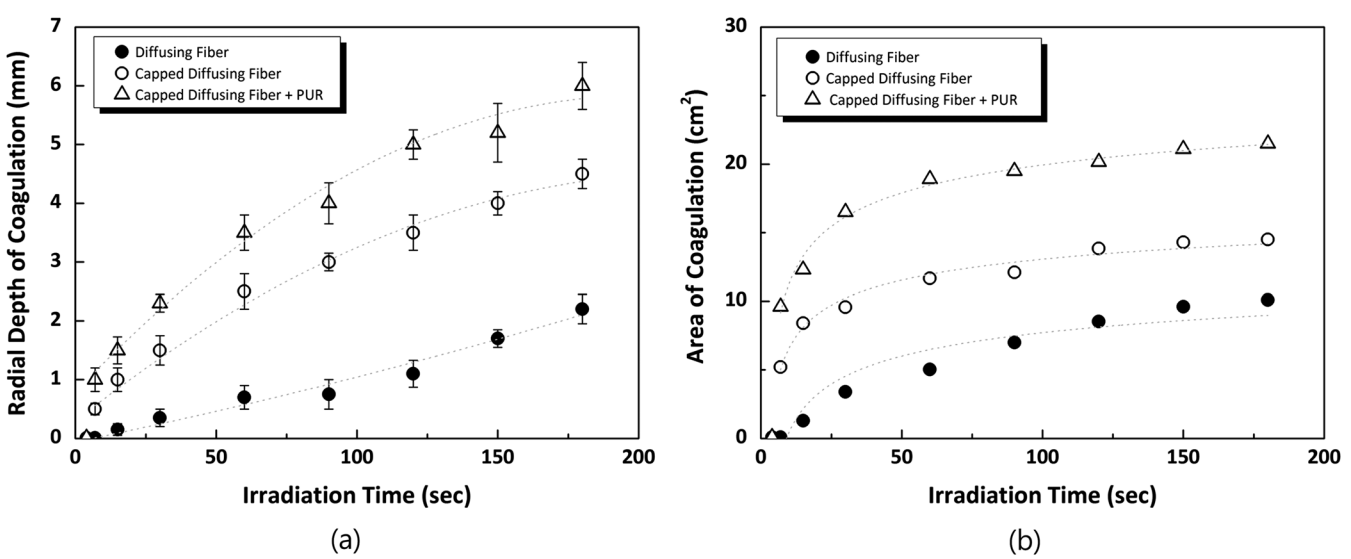

Fig. 5 Quantitative evaluation of coagulated tissue as function of irradiation time: (a) radial depth (mm) of coagulation and (b) area (cm^2) of coagulation with three experimental conditions (diffusing, capped diffusing, and capped diffusing fiber along with polyurethane layer).

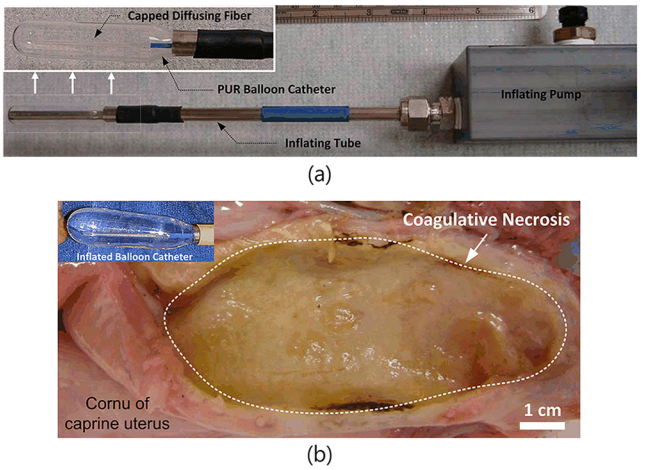

Fig. 6 Balloon catheter-combined diffusing fiber for endometrial coagulation: (a) prototype design consisting of capped diffusing fiber balloon catheter, inflating tube, and pump and (b) caprine uterine horn tissue coagulated *in vivo* with prototype device.

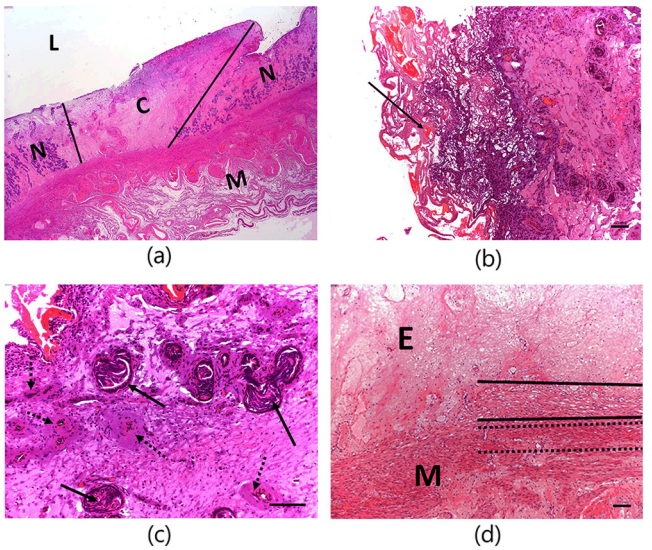

Fig. 7 H&E-stained histological images of caprine uterine tissue 2 h after *in vivo* coagulation testing: (a) uterine horn (20×, L: lumen, C: coagulated endometrium, N: normal endometrial layer, M: myometrium), (b) focal site of protein coagulum (100×; bar = 10 mm), (c) coagulated endometrial glands (200×; bar = 10 mm), and (d) myometrium adjacent to treated lesion (100×, E: endometrium and M:myometrium; bar = 10 mm).

cadaver study versus 1.5 cm for *in vivo* study) and thereby, its 30% higher irradiance (i.e., 4.2 W/cm^2 for cadaver study versus 3.2 W/cm^2 for *in vivo* study). Figure 8(b) shows a sequence of endometrial coagulation with the prototype balloon catheter-assisted diffusing device. Prior to the treatment, the device securely held the uterus [far left image in Fig. 8(b)], and during the treatment (middle image), the scattered photons (532 nm) were visualized through the tissue, indicating the ongoing intra-operation. According to posttreatment (far right image), the overall thickness of coagulation necrosis was found to be 2.6 ± 0.6 mm ($n = 12$). The coagulation thickness slightly thinner than the *in vivo* results ($p = 0.50$) indirectly evidenced that the adjusted dosimetry for the cadaver study (i.e., 4.2 W/cm^2 and 20 s irradiation) was able to induce photocoagulation effects equivalent to those for the *in vivo* studies (i.e., 3.2 W/cm^2 and 30 s irradiation).

4 Discussion

Spatial distribution of photons between diffusing and capped diffusing fibers were simulated and compared at various distances in Fig. 3. The current simulation models used a planar detector that displayed the gradient distribution of irradiance only in 2-D. However, the inherent anatomy of human uterus can be rather circular or doughnut shape.[20] In turn, the intensity of the incident laser light can be constantly maintained along x-axis (horizontally) as the laser light is uniformly irradiated on the curved uterine wall at a constant distance with the aid of a concentric balloon-catheter. Unlike Fig. 3(b), the slope of the wings on the horizontal position would flatten out if one utilized the circular detector with the equivalent curvature that the diffuser had. Future investigations will be conducted to verify the physical distribution of the incident irradiance along the curvature of the uterine wall. In addition, the role of the glass cap layer will be studied to optimize the light distribution in light of layer thickness, curvature, and refractive index of the glass cap.

A capped diffusing fiber with PUR induced rapid and wide tissue coagulation as shown in Figs. 4–6. Both the wide distribution of the incident photons from the glass cap (Fig. 3) and inhomogeneous illumination from the diffuser on the tissue surface [Fig. 2(b)] could be responsible for lateral thermal expansion particularly with longer irradiation times, leading to the wide coagulation. It is also conceived that the enhanced coagulation was associated with thermal insulation of the PUR material.[30] As the target tissue heated up upon light absorption, the PUR layer behaved as a thermal barrier to trap and accumulate the laser-induced heat inside the tissue. An insignificant amount of heat could barely diffuse through the PUR layer, in that thermal conductivity of PUR is almost 25-fold higher than that of water (i.e., 0.023 W/m · K for PUR versus 0.630 W/m · K for water at 37°C).[30,31] In an attempt to ensure the efficacy and safety of the enhanced photocoagulation, numerical simulation on temperature development and distribution in tissue is underway to optimize the design dimension and material properties (optical, thermal, and mechanical) of PUR. For the sake of experimental validation, tissue temperature during laser irradiation with the optical diffuser will also be quantified with thermocouples embedded in tissue.

Based upon the assumption that an endometrial layer was 3 mm thick, the irradiation time for *in vivo* experiments was selected as 30 s to generate the coagulation thickness comparable to the endometrium thickness [Fig. 5(a)]. Although the typical thickness of the endometrial layer in human uterus is approximately 5 mm,[20] the uterine wall can become thinned-out owing to the expansion of the uterus during laser surgery. Thus, to ensure that the laser light solely ablates the endometrium without any thermal damage to the subjacent myometrium, the wall thickness was conservatively assumed to be 3 mm, roughly corresponding to the irradiation time of 30 s as shown in Fig. 5(a). In fact, the *in vivo* results evidenced that the measured coagulation thickness was comparable to 3 mm (Fig. 7). Thus, the conservative assumption on the distended uterine wall must have been valid and safe enough to protect the layer underneath the endometrium. Chronic response of uterine tissue (three day survival) will be further evaluated to investigate the histopathologic evolution of the treated uterine tissue as well as its potential healing patterns.

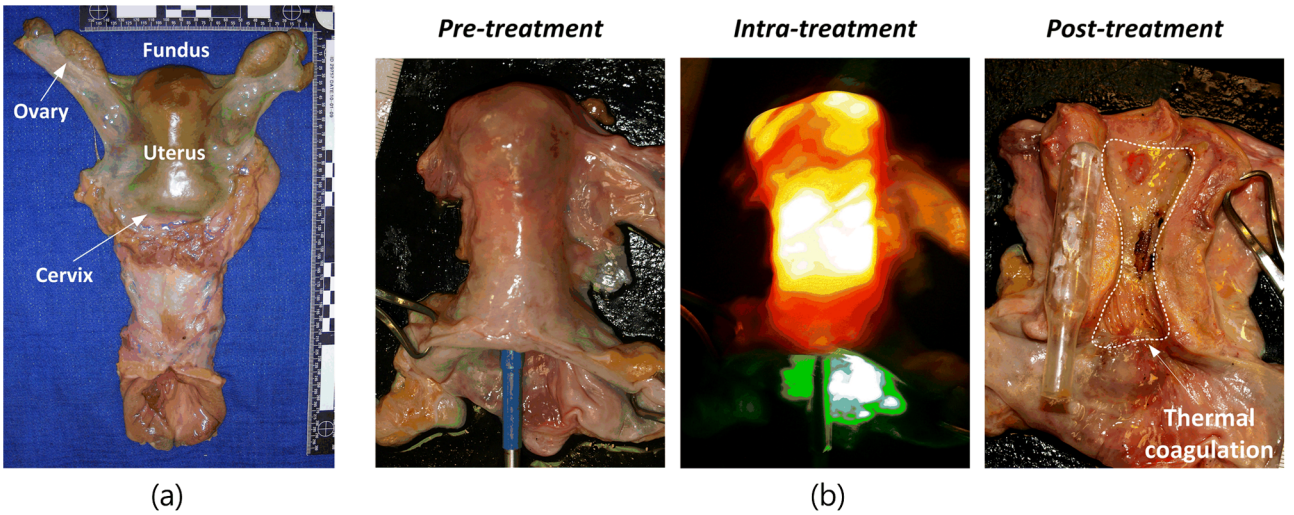

Fig. 8 Cadaver study with prototype diffusing optical device: (a) human uterus harvested from 59-year-old patient after radical hysterectomy and (b) sequence of endometrial coagulation with diffusing device (pre-, intra-, and posttreatment).

Considering a typical uterus volume,[32] the estimated average irradiance on the entire uterus surface area (i.e., 88 cm^2 assuming a uterine cavity as a frustum of right circular cone) would be 1.3 W/cm^2 under 120-W application. The estimated value is approximately 70% lower than the irradiance (4.2 W/cm^2) used for the cadaver study; thus, one may need a longer irradiation time in order to achieve the comparable coagulation thickness. Moreover, since the uterus is a closed volume, diffuse reflection from the uterine wall (i.e., integrating sphere effect) could take place to uniformly distribute the diffusely scattered light, subsequently expanding thermal diffusion.[33] Accordingly, one may have to take into account the effect of diffuse scattering on the uterine wall in an attempt to determine the appropriate irradiation time for clinical tests. It was also noted that a certain part of the treated tissue was superficially carbonized [Fig. 8(c)]. Since the diffusing fiber was attached only to the distal end of the inflating tube, insecure location of the diffusing fiber tip could be responsible for the unwanted carbonization as the fiber tip freely moved around in the distended balloon catheter even during/after irradiation. Furthermore, under the current study, 120-W input power was applied to yield enough irradiance through the diffusing tip and to entail tissue coagulation. Although high laser power has clinically been used,[34] undesirable fiber failure would be detrimental to peripheral tissues, organs, and eventually patients. Thus, precautions such as fiber shield and optical feedback system should be considered for the new design to ensure safety during laser treatment.

Since a cylindrical shape of the balloon catheter was used to make the prototype, the entire surface of the endometrium hardly achieved the uniform coagulation. Moreover, the anatomy of human uterus seems triangular rather than cylindrical (on the sagittal plane). In an attempt to resolve the current challenges such as free movement of fiber tip and diverse uterus geometry, the new design for the optical device has been suggested and under investigation (Fig. 9). Firstly, a small holder is placed in the ceiling inside the balloon (to fix the position of the diffusing fiber tip, so the optical diffuser can stay in the center of the catheter even during device deployment and laser irradiation. Secondly, the shape of the balloon catheter is redesigned to be triangular, so the entire balloon can increase the light coverage of the endometrium surface. Finally, along with the new geometry of the balloon, the light distribution should change by providing the gradient of light intensity from different shapes of scattering segments on the fiber surface. In other words, more light can be concentrated on the upper part of the balloon, so the entire irradiance can be uniform over the inner surface of the balloon catheter. Further preclinical and clinical evaluations will validate the performance of the new optical device for endometrial treatment.

The current study demonstrated the laser irradiation time on the order of seconds to treat endometrial cell layers (Figs. 4, 6, and 8). Although the results may satisfy the clinical unmet need for quick treatment (~*a* few mins) raised by gynecologists and patients,[3,4] the real clinical situations would take much longer (on the order of minutes) to complete treatment due to various sizes of distended human uterus and resultantly lower irradiance on the uterine wall. From the safety perspective, the input power lower than the current power used (120 W) would be more desirable for clinical treatments to prevent any adverse events caused by fiber failure. Accordingly, the new design of the diffuser tip should take into consideration ways to optimize laser and fiber parameters such as low input power, high transmission, and uniformity of light distribution. Furthermore, in an attempt to enhance both clinical efficacy and safety, other minimally

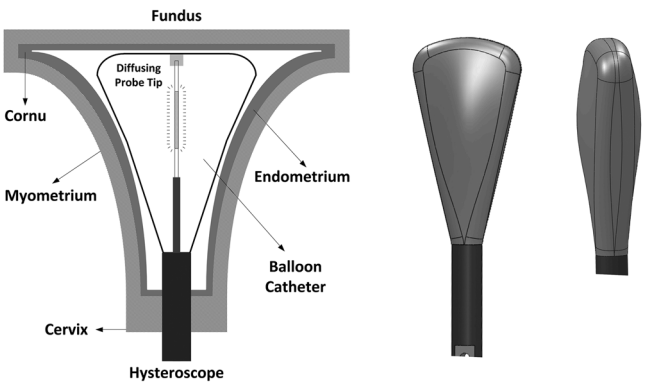

Fig. 9 New design of balloon catheter-assisted diffusing optical device. Note the fixed fiber tip (left) and geometrical modifications (right) emulating anatomical features of uterus.

invasive techniques such as PDT have also been studied for treating AUB.[29,35] Particularly, as PDT successfully induced endometrial destruction in a rat model, the newly proposed optical device can be compared and evaluated with PDT in terms of treatment performance and safety. Additional investigations will thereby be planned to verify the feasibility of incorporating two minimally invasive treatments into one potential therapeutic tool to amplify clinical outcomes.

5 Conclusion

The feasibility of the newly designed diffusing optical device was demonstrated for endometrial treatment. Due to the wide distribution of photons with high irradiance, the new optical diffuser was incorporated into a balloon catheter facilitated photocoagulation globally, compared to other minimally invasive techniques. The optical response of uterine tissue to 532 nm irradiation confined tissue coagulation to endometrial cell layers without any thermal injury to myometrium, unlike Nd:YAG lasers that cause deep coagulation necrosis. The uniform and rapid development of coagulation (2 to 3 mm thick) evidenced that the balloon catheter-based optical diffuser can be exploited to treat heavy menstrual bleeding as a simple and safe therapeutic device. Further development of the proposed design may provide a more efficient and safer tool for gynecologists to treat menorrhagia as well as other uterine diseases in a minimally invasive way and eventually to minimize postoperative complications.

Acknowledgments

The authors thank J. Guth and E. Koullick for fiber fabrication and D. Jebens for valuable assistance with optical simulation. This research was supported by Basic Science Research Program through the National Research Foundation of Korea (NRF) funded by the Ministry of Education, Science and Technology (2012R1A1A1012965).

References

1. S. B. Fazio and A. N. Ship, "Abnormal uterine bleeding," *South. Med. J.* **100**(4), 376–382 (2007).
2. M. G. Munro, "Endometrial ablation for heavy menstrual bleeding," *Curr. Opin. Obstetr. Gynecol.* **17**(4), CD000329 (2005).
3. A. Lethaby and M. Hickey, "Endometrial destruction techniques for heavy menstrual bleeding: a Cochrane review," *Hum. Reprod.* **17**(11), 2795–2795 (2002).
4. A. Lethaby et al., "Endometrial resection/ablation techniques for heavy menstrual bleeding," *Cochrane Database Syst. Rev.* **4**, CD001501 (2009).
5. J. V. Pinkerton, "Pharmacological therapy for abnormal uterine bleeding," *Menopause* **18**(4), 453–461 (2011).
6. A. Lethaby et al., "Endometrial resection and ablation versus hysterectomy for heavy menstrual bleeding," *Cochrane Database Syst. Rev.* **2**, CD000329 (2000).
7. C. Bain, K. G. Cooper, and D. E. Parkin, "Microwave endometrial ablation versus endometrial resection: a randomized controlled trial," *Obstetr. Gynecol.* **99**(6), 983–987 (2002).
8. J. Marjoribanks, A. Lethaby, and C. Farquhar, "Surgery versus medical therapy for heavy menstrual bleeding," *Cochrane Database Syst. Rev.* **2**, CD003855 (2009).
9. R. Garside, K. Stein, K. Wyatt, and A. Round, "Microwave and thermal balloon ablation for heavy menstrual bleeding: a systematic review," *BJOG* **112**(1), 12–23 (2005).
10. J. P. Daniels et al., and International heavy menstrual bleeding IPD meta-analysis collaborative group, "Second generation endometrial ablation techniques for heavy menstrual bleeding: network meta-analysis," *BMJ* **344**, e2564 (2012).
11. Z. Amin, "Diode lasers: experimental and clinical review," *Lasers Med. Sci.* **10**(3), 157–163 (1995).
12. C. Rosenberg et al., "Endometrial laser ablation in rabbits: a comparative study of three laser types," *Lasers Surg. Med.* **10**(1), 66–73 (1990).
13. M. Ueki et al., "Experimental and clinical studies on balloon laserthermia using Nd: YAG laser for uterine endometrial cancer," *Lasers Surg. Med.* **18**(2), 178–186 (1996).
14. J. C. Mizeret and H. E. van den Bergh, "Cylindrical fiber optic light diffuser for medical applications," *Lasers Surg. Med.* **19**(2), 159–167 (1996).
15. D. M. Cromeens et al., "Visual laser ablation of the canine prostate with a diffusing fiber and an 805-nanometer diode laser," *Lasers Surg. Med.* **19**(2), 135–142 (1996).
16. P. J. Dwyer et al., "Optical integrating balloon device for photodynamic therapy," *Lasers Surg. Med.* **26**(1), 58–66 (2000).
17. L. M. Vesselov, W. Whittington, and L. Lilge, "Performance evaluation of cylindrical fiber optic light diffusers for biomedical applications," *Lasers Surg. Med.* **34**(4), 348–351 (2004).
18. L. Vesselov, W. Whittington, and L. Lilge, "Design and performance of thin cylindrical diffusers created in Ge-doped multimode optical fibers," *Appl. Opt.* **44**(14), 2754–2758 (2005).
19. S. L. Jacques, "Laser-tissue interactions, photochemical, photothermal, and photomechanical," *Surg. Clin. North Am.* **72**(3), 531–558 (1992).
20. E. Ramsey, "Anatomy of the human uterus," in *The Uterus*, T. Chard and J. G. Grudzinskas, Eds., pp. 18–29, Cambridge University Press, Cambridge, UK (1994).
21. H. Klank, J. P. Kutter, and O. Geschke, "CO_2-laser micromachining and back-end processing for rapid production of PMMA-based microfluidic systems," *Lab Chip* **2**(4), 242–246 (2002).
22. D. C. O'Brien et al., "High data-rate optical wireless communications in passenger aircraft: Measurements and simulations," in *Communication Systems, Networks and Digital Signal Processing, 2008, 6th International Symposium*, IEEE (2008).
23. S. Thomsen, "Pathologic analysis of photothermal and photomechanical effects of laser-tissue interactions," *Photochem. Photobiol.* **53**(6), 825–835 (1991).
24. A. Vogel and V. Venugopalan, "Mechanisms of pulsed laser ablation of biological tissues," *Chem. Rev.* **103**(2), 577–644 (2003).
25. Y. Kawase et al., "*In vivo* volumetric analysis of coronary stent using optical coherence tomography with a novel balloon occlusion-flushing catheter: A comparison with intravascular ultrasound," *Ultrasound Med. Biol.* **31**(10), 1343–1349 (2005).
26. S. Mobini, "Cosmetic dehorning of adult goats," *Small Ruminant Res.* **5**(1–2), 187–191 (1991).
27. K. M. Dyce, W. O. Sack, and C. J. G. Wensing, *Textbook of Veterinary Anatomy*, WB Saunders Co., St. Louis, Missouri (1987).
28. G. Shea, "Textbook of veterinary anatomy," *Aust. Vet. J.* **81**(5), 270–270 (2003).
29. A. A. Krzemien et al., "Evaluation of novel nonlaser light source for endometrial ablation using 5-aminolevulinic acid," *Lasers Surg. Med.* **25**(4), 315–322 (1999).
30. J. Kuhn et al., "Thermal transport in polystyrene and polyurethane foam insulations," *Int. J. Heat Mass Transfer* **35**(7), 1795–1801 (1992).
31. J. W. Wu, W. F. Sung, and H. S. Chu, "Thermal conductivity of polyurethane foams," *Int. J. Heat Mass Transfer* **42**(12), 2211–2217 (1999).
32. T. Tsilchorozidou and G. S. Conway, "Uterus size and ovarian morphology in women with isolated growth hormone deficiency, hypogonadotrophic hypogonadism and hypopituitarism," *Clin. Endocrinol.* **61**(5), 567–572 (2004).
33. W. M. Star et al., "Light dosimetry for photodynamic therapy by whole bladder wall irradiation," *Photochem. Photobiol.* **46**(5), 619–624 (1987).
34. R. S. Malek et al., "Photoselective vaporization prostatectomy: experience with a novel 180 W 532 nm lithium triborate laser and fiber delivery system in living dogs," *J. Urol.* **185**(2), 712–718 (2011).
35. R. A. Steiner et al., "Photosensitization of the rat endometrium following 5-Aminolevulinic acid induced photodynamic therapy," *Lasers Surg. Med.* **18**(3), 301–330 (1996).